

High-temperature magnetoelectricity of terbium aluminum borate: The role of excited states of the rare-earth ion

A. M. Kadomtseva,^{1,*} Yu. F. Popov,¹ G. P. Vorob'ev,¹ N. V. Kostyuchenko,^{2,3} A. I. Popov,^{2,4} A. A. Mukhin,² V. Yu. Ivanov,² L. N. Bezmaternykh,⁵ I. A. Gudim,⁵ V. L. Temerov,⁵ A. P. Pyatakov,^{1,2} and A. K. Zvezdin^{2,3}

¹Physics Department, M. V. Lomonosov Moscow State University, MSU, Leninskie Gori, Moscow 119992, Russia

²Prokhorov General Physics Institute, Russian Academy of Sciences, Moscow, Russia

³Moscow Institute of Physics and Technology (State University), Moscow, Russia

⁴National Research University of Electronic Technology MIET, Zelenograd, Russia

⁵L. V. Kirensky Institute of Physics Siberian Branch of RAS Krasnoyarsk 660036, Russia

(Received 13 September 2013; revised manuscript received 3 January 2014; published 21 January 2014)

Recently discovered magnetoelectricity in the rare-earth aluminum borates $\text{RAl}_3(\text{BO}_3)_4$ has attracted attention due to the large values of magnetoinduced electric polarization. We have observed for the first time the magnetoelectric polarization in $\text{TbAl}_3(\text{BO}_3)_4$ exhibiting anomalous temperature dependence: an electric polarization induced by in-plane magnetic field ($P \parallel a, H \perp c$ axis) which is small at low temperatures (4 K), remarkably increases by almost an order of magnitude at high temperatures (150–300 K). The observed nonmonotonic temperature behavior of the field-induced polarization, including a change of sign at ~ 65 –70 K, is attributed to the competition of the ground and excited crystal-field states of Tb^{3+} ions. Quantum theory analysis, involving the combination of analytical and numerical methods, has enabled us to quantitatively describe the observed magnetic and magnetoelectric properties of $\text{TbAl}_3(\text{BO}_3)_4$.

DOI: 10.1103/PhysRevB.89.014418

PACS number(s): 75.85.+t

I. INTRODUCTION

Multiferroic materials with coexisting magnetic and electric ordering [1] have attracted ever-growing attention over recent years. They have been known for more than half a century [2,3], but the major progress in the understanding of these media was achieved in the last ten years [4–8] with the advent of new experimental characterization techniques and computational methods. Nevertheless, the search for room temperature materials with strong magnetoelectric coupling is still on the agenda. The conventional phenomenological approach based on symmetry analysis can only predict the presence or absence of the effect and does not provide its value as well as the detailed dependencies of electric polarization on magnetic field or temperature.

The discovery of high electric polarization induced by magnetic ordering in multiferroic rare-earth iron borates [9,10] with the general formula $\text{RFe}_3(\text{BO}_3)_4$ (R—rare-earth ion) stimulated the search for the magnetoelectric effect in isostructural compounds like aluminum borates $\text{RAl}_3(\text{BO}_3)_4$ [11,12] that were previously considered mainly as optical and magneto-optical materials [13,14].

Despite the absence of magnetic ordering in the aluminum borates, they demonstrate significant electric polarization in strong magnetic fields (for holmium aluminum borate the magnetically induced polarization exceeds $3000 \mu\text{C}/\text{m}^2$ in a field ~ 100 kOe [11]). These compounds are convenient model objects which allow to clarify the contribution of rare-earth ions to the magnetoelectric coupling (due to the absence of iron ions and the f - d exchange interaction). The magnetoelectric effect in aluminum borates similar to iron borates is due to the rare-earth f ions [16,17]. The single-ion mechanism

dominates over the two-ion one because of a large orbital moment, weak suppression of the orbital moment by a low-symmetry crystal field, and a weak exchange interaction (as compared to the d - d and f - d one) between the rare-earth f ions.

In this paper we study both experimentally and theoretically the magnetic and magnetoelectric properties of $\text{TbAl}_3(\text{BO}_3)_4$. Electric polarization has not yet been observed in this compound [12], probably due to strong crystal field effects resulting in a large uniaxial magnetic anisotropy, which hamper the field-induced electric polarization at low temperatures. On the other hand, one could expect a manifestation of the magnetoelectric effect at high temperatures (up to ambient), an effect that has already been observed in terbium iron borate [18], and which could be interesting for possible applications. Our measurements in high pulsed magnetic fields reveal that the electric polarization in $\text{TbAl}_3(\text{BO}_3)_4$ possess an unusual temperature dependence, which we successfully describe by quantum theory of the magnetoelectric effect taking into account the spectrum of Tb^{3+} ions in both the crystal and magnetic fields.

II. EXPERIMENTAL RESULTS

$\text{TbAl}_3(\text{BO}_3)_4$ single crystals were grown by the group flux method on seeds, which is described in detail in Ref. [15]. The magnetic measurements were performed by means of a superconducting quantum interference device (SQUID) magnetometer (Quantum Design) in magnetic fields of up to 50 kOe. The electric polarization P was studied in pulsed magnetic fields up to 250 kOe at temperatures from 4.2 to 300 K. Epoxy resin electrodes with conducting filler were deposited on the sample facets normal to the direction of measured polarization. The induced charge was measured by an electrometer. The time of charge leakage from the sample

*With great sadness we announce that Dr. A. M. Kadomtseva passed away during the preparation of this paper.

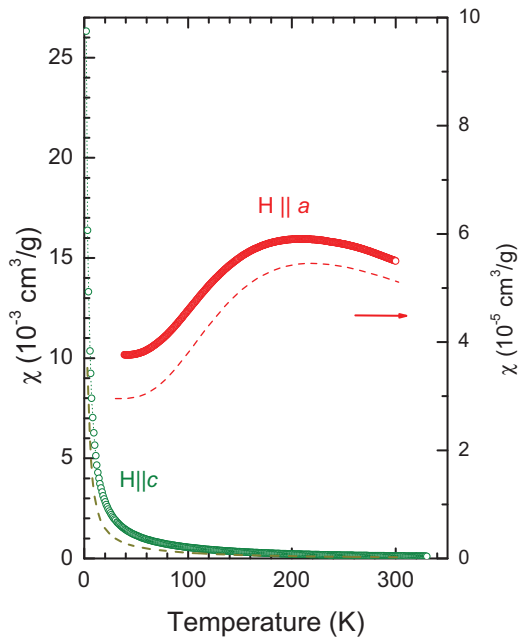


FIG. 1. (Color online) Temperature dependencies of the magnetic susceptibility along *c* and *a* axes. Points—experimental data, dashed lines—the results of calculations using formula (4) at $H = 1$ kOe.

for magnetic field pulse durations of $t_p \sim 10^{-2}$ s used in our experiments was two or three orders of magnitude longer than the measurement time, ensuring the reliability of the results (see details in Ref. [19]).

The temperature dependence of magnetic susceptibilities measured at 1 kOe (Fig. 1) and magnetization curves (Fig. 2) shows strong magnetic anisotropy along the *a* and *c* axes. The magnetic susceptibility $\chi_c(T)$ reveals a significant increase and Curie-Weiss-like behavior up to the lowest temperatures while the $\chi_a(T)$ becomes almost constant at $T < 50$ K, exhibits a

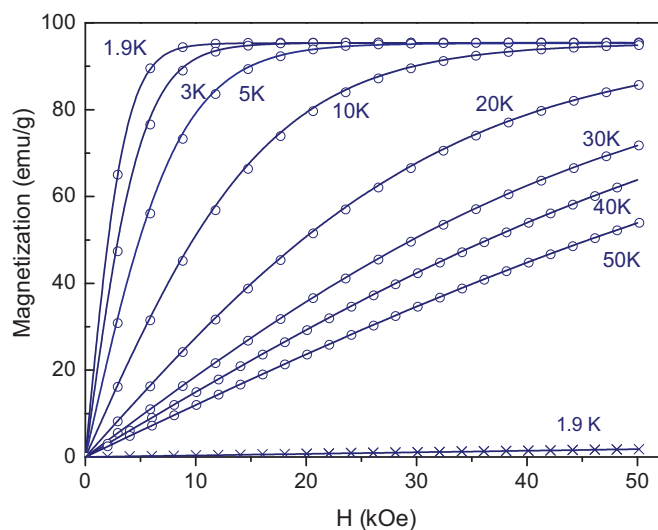


FIG. 2. (Color online) Experimental and theoretical magnetization dependencies on magnetic field at different temperatures. Solid lines—the results of calculations using formula (3). Symbols—experimental data, \circ — $H||c$, \times — $H||a$.

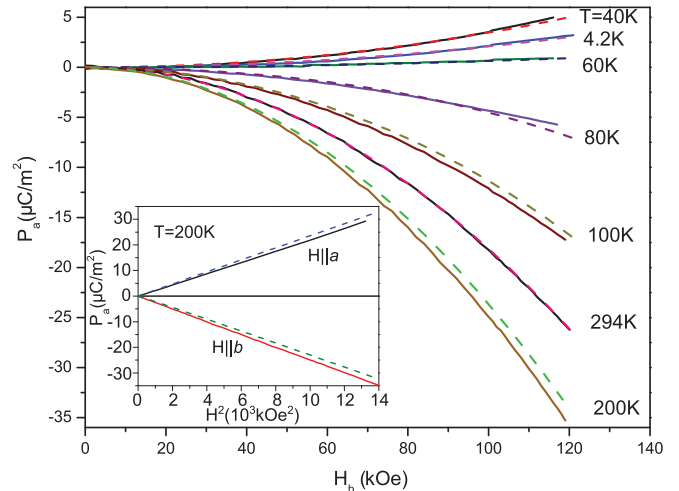


FIG. 3. (Color online) Experimental and theoretical dependencies of the electric polarization $P_a(H_b)$ on magnetic field at different temperatures. Insert: Comparison of the electric polarization behavior in the transverse $P_a(H_b)$ and longitudinal $P_a(H_a)$ geometries reflecting its symmetry properties $P_a \sim H_a^2 - H_b^2$. Dashed lines—the results of calculations using formula (10) at $d_2^2 = -1.25 \times 10^5 \mu\text{C}/\text{m}^2$, $d_2^4 = -2.12 \times 10^5 \mu\text{C}/\text{m}^2$, solid lines—experimental data.

maximum at ~ 200 K and Curie-Weiss law behavior only at the high temperatures. The observed strong anisotropy of the susceptibility at the low T ($\chi_c/\chi_a \sim 700$ at $T = 1.9$ K) allows to consider the Tb^{3+} ions as Ising ones and clearly indicates an essential role of the crystal field effects in $\text{TbAl}_3(\text{BO}_3)_4$. The low-temperature value of $\chi_a \approx (3.5 \pm 0.5)10^{-5} \text{cm}^3/\text{g}$ was found from several separate measurements due to the high sensitivity of $\chi_a(T)$ to any small misalignment of the magnetic field from the *a* axis and the admixture of the large $\chi_c(T)$ component. A saturation of the magnetization along the Ising *c* axis at the low temperature ($\sim 8\mu_B/Tb$) occurs in the magnetic fields ≈ 10 kOe (Fig. 2). In the perpendicular direction (*a* axis) the magnetization is much smaller, it exhibits a practically linear dependence on magnetic field and its weak temperature dependence indicates that it is of Van-Vleck origin.

Now let us consider the magnetoelectric properties of $\text{TbAl}_3(\text{BO}_3)_4$. Our measurements at the lowest temperatures (≈ 4.2 K) revealed a small field-induced electric polarization $P_a(H_b)$ along the *a* axis for $H||b$ exhibiting quadratic field dependence and reaching the value only $\approx 2\text{--}3 \mu\text{C}/\text{m}^2$ at 120 kOe (Fig. 3). The polarization $P_a(H_b, T)$ shows nonmonotonic behavior. With the increase in temperature, it changes its sign at $T \sim 65\text{--}70$ K and passes via a broad maximum of its absolute value ($\approx 25 \mu\text{C}/\text{m}^2$) at the high-temperature range of (150–200 K) close to ambient. Similar behavior was also observed for the polarization in longitudinal geometry $P_a(H_a, T)$ (Fig. 4), which had an opposite sign (see the insert in Fig. 3) in good agreement with the symmetry relations $P_a \sim (H_a^2 - H_b^2)$ [10]. Temperature dependencies of the electric polarization P_a induced by the magnetic field 100 kOe along *a* and *b* axes are shown in Fig. 5 and clearly illustrate the aforementioned features of the temperature evolution of the polarization and the important role of the crystal field effects

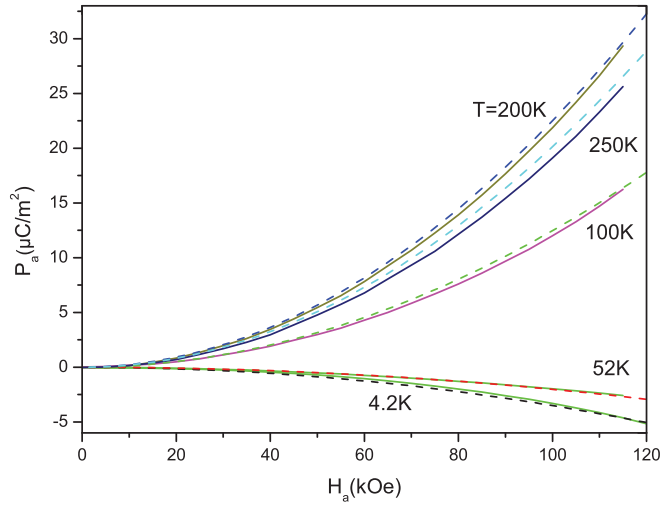


FIG. 4. (Color online) Dependencies of polarization P_a on the external magnetic field directed along the a axis. Dashed lines—the results of calculations using formula (10) at $d_2^2 = -1.25 \times 10^5 \mu\text{C}/\text{m}^2$, $d_2^4 = -2.12 \times 10^5 \mu\text{C}/\text{m}^2$, solid lines—experimental data.

for Tb^{3+} ions. Indeed, at low temperatures the strong (Ising) magnetic anisotropy of the Tb^{3+} ions (in particular, small Van-Vleck susceptibility in the basal plane) hinders the electric polarization induced by the field H . The observed change of its sign and the increase of its absolute value at higher temperatures could be naturally explained by the increase in the population of the excited states.

III. THEORY AND DISCUSSION

A. Crystal-field Hamiltonian, energy levels, and wave functions of the terbium ion

The environment symmetry of the rare-earth ions in aluminum borates is described by the point symmetry group D_3 .

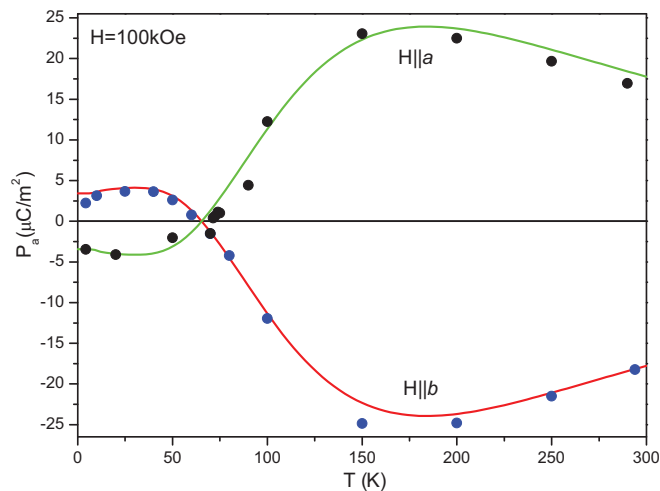


FIG. 5. (Color online) Temperature dependencies of the electric polarization induced by the magnetic field 100 kOe along the a and b axes. Solid lines—the results of calculations using formula (10) at $d_2^2 = -1.25 \times 10^5 \mu\text{C}/\text{m}^2$, $d_2^4 = -2.12 \times 10^5 \mu\text{C}/\text{m}^2$, points—experimental data.

TABLE I. The split of ground multiplet in a crystal field.

n	$\tilde{E}_n, \text{cm}^{-1}$	ψ_n
1	0.00	$0.701(6\rangle + -6\rangle) + 0.093i(3\rangle + -3\rangle) - 0.030 0\rangle$
2	0.34	$-0.702(6\rangle - -6\rangle) - 0.088i(3\rangle - -3\rangle)$
3	243.93	$0.862i -5\rangle - 0.481 -2\rangle - 0.142i 1\rangle - 0.073 4\rangle$
4	243.93	$-0.073 -4\rangle - 0.142i -1\rangle - 0.481 2\rangle + 0.862i 5\rangle$
5	288.02	$0.065(6\rangle + -6\rangle) - 0.352i(3\rangle + -3\rangle) + 0.862 0\rangle$
6	294.45	$0.568 -4\rangle + 0.799i -1\rangle + 0.027 2\rangle + 0.196i 5\rangle$
7	294.45	$0.196i -5\rangle + 0.027 -2\rangle + 0.799i 1\rangle + 0.568 4\rangle$
8	430.72	$0.452i -5\rangle + 0.832 -2\rangle + 0.082i 1\rangle - 0.311 4\rangle$
9	430.72	$-0.311 -4\rangle + 0.082i -1\rangle + 0.832 2\rangle + 0.452i 5\rangle$
10	430.73	$-0.088(6\rangle - -6\rangle) + 0.702i(3\rangle - -3\rangle)$
11	466.60	$0.759 -4\rangle - 0.578i -1\rangle + 0.275 2\rangle + 0.122i 5\rangle$
12	466.60	$0.122i -5\rangle + 0.275 -2\rangle - 0.578i 1\rangle + 0.759 4\rangle$
13	476.34	$-0.069(6\rangle + -6\rangle) + 0.606i(3\rangle + -3\rangle) + 0.506 0\rangle$

The Hamiltonian of the crystal field in the frame with C_3 axis along z (c) and C_2 axis along x (a) can be presented in the following form:

$$\mathcal{H}_{\text{CF}} = B_0^2 C_0^{(2)} + B_0^4 C_0^{(4)} + B_0^6 C_0^{(6)} + i B_{-3}^4 [C_{-3}^{(4)} + C_3^{(4)}] + i B_{-3}^6 [C_{-3}^{(6)} + C_3^{(6)}] + B_6^6 [C_{-6}^{(6)} + C_6^{(6)}]. \quad (1)$$

In this equation $C_q^{(k)} = \sum_i C_q^{(k)}(i)$, where $C_q^{(k)}(i)$ are single electron irreducible tensor operators.

The crystal-field parameters for Tb^{3+} are [20]

$$B_0^2 = 581 \text{ cm}^{-1}, \quad B_0^4 = -1254 \text{ cm}^{-1}, \quad B_0^6 = -161 \text{ cm}^{-1}, \\ B_4^3 = 815 \text{ cm}^{-1}, \quad B_4^5 = 180 \text{ cm}^{-1}, \quad B_6^6 = 41 \text{ cm}^{-1}. \quad (2)$$

In the study of the magnetization process, it is sufficient to consider only the ground-state multiplet of the terbium ion. The energy levels and the wave functions of the ground 7F_6 multiplet of the Tb^{3+} ion in the crystal field calculated with the exclusion of the admixture of the overlying multiplets are presented in Table I.

B. Magnetization and susceptibility

The magnetization and magnetic susceptibility are determined by

$$\mathbf{M} = -N g_J \mu_B \times \frac{\sum_i \langle \psi_i | \hat{J} | \psi_i \rangle \exp(-E_i/kT)}{\sum_i \exp(-E_i/kT)}, \quad (3)$$

$$\chi_{\alpha\beta} = \frac{\partial M_\alpha}{\partial H_\beta}, \quad (4)$$

where E_i and ψ_i are, respectively, the energy levels and the wave functions of the Tb^{3+} ions in the crystal field and external magnetic field determined by the Hamiltonian $\mathcal{H} = \mathcal{H}_{\text{CF}} + g_J \mu_B \hat{J} H$, where J is the total angular momentum of the ground Tb^{3+} multiplet, g_J is the Lande splitting factor, μ_B is the Bohr magneton, and N is the number (concentration) of the Tb^{3+} ions.

A comparison of numerically calculated magnetic susceptibility along and perpendicular to the C_3 axis as well as the magnetization curves with the corresponding experimental data are shown in Figs. 1 and 2. The theory is in agreement

with the experiment, thus confirming a reasonable values of the crystal field parameters B_n^k .

C. Magnetoelectric effect

The electronic mechanism of the magnetoelectric effect has been already developed for rare-earth iron borates in Refs. [21,22]. Here we apply the same approach to terbium aluminum borate.

Suppose an external electric field is applied to a crystal. Then the actual terms of Hamiltonian will be written as

$$\mathcal{H} = -\mathbf{d} \cdot \mathbf{E} + \mathcal{H}_{\text{CF}}^{\text{odd}}. \quad (5)$$

Here $\mathbf{d} = -e \sum_{k=1}^n \mathbf{r}_k$ is the dipole moment of the ion with n electrons in the $4f$ shell. $\mathcal{H}_{\text{CF}}^{\text{odd}}$ is the odd operator of the crystal field.

The corrections to the energy levels of the ion, which are linear in the applied electric field, emerge in the second order of perturbation theory with a small parameter $||\mathcal{H}||/W$, where $||\mathcal{H}||$ is the norm of the operator \mathcal{H} in Eq. (5), and W is the difference between the ground state and the average energy of the excited electron configurations (usually $W \sim 10^5 \text{ cm}^{-1}$ for rare-earth ions).

We can find an expression for the magnetoelectric operator of a rare-earth aluminum borate using the genealogical coupling scheme of construction of the electron wave functions and a quantum theory of the angular momentum [23]

$$\mathcal{H}_{me} = -\mathbf{E}\mathbf{D} = -(E_x D_x + E_y D_y + E_z D_z), \quad (6)$$

where $E_{\pm} = (E_x \pm iE_y)/\sqrt{2}$, D_{α} ($\alpha = x, y, z$) are the operators for the components of the effective electric dipole moment of a rare-earth ion, which can be presented in the form of multipole expansion of the rare-earth ion [22,23]

$$D_{\pm} = \frac{(D_x \pm iD_y)}{\sqrt{2}} = \sum_{p=2,4,6} b_2^p \hat{C}_{\mp 2}^p + \sum_{p=4,6} b_4^p \hat{C}_{\pm 4}^p, \\ D_z = b_3^4 (\hat{C}_3^4 - \hat{C}_{-3}^4) + b_3^6 (\hat{C}_3^6 - \hat{C}_{-3}^6). \quad (7)$$

The constants b_q^p contain contributions of the electronic [$b_q^p(e)$] and ionic [$b_q^p(i)$] mechanisms to the polarization [23]. The values of $b_q^p(e)$ are expressed through odd crystal field components [23] which are not known with a sufficient degree of precision. We are aware of only one article [24] where the parameters of the odd crystal field have been calculated for Pr^{3+} in praseodymium iron borate based on the point-charge model. In addition to the parameters of the odd crystal field, the contribution of the ion mechanism depends on force constants c_{α} (see Ref. [23]) for which the values are currently unknown. Generally speaking, the values b_q^p can be treated as phenomenological parameters of the Hamiltonian \mathcal{H}_{me} and can be determined by fitting the experimental data.

Using this approach, the magnetoelectric contribution to the free energy of the crystal is equal to

$$\mathcal{F}_{me} = -N\mathbf{E}\langle\mathbf{D}\rangle. \quad (8)$$

The symbol $\langle \dots \rangle$ signifies the thermodynamic averaging over wave functions of a rare-earth ion. Obviously, an average of the D_{α} operators over the states of Tb^{3+} in the crystal field only (see Table I) leads to $\langle D_{\alpha} \rangle = 0$. Therefore, one must take

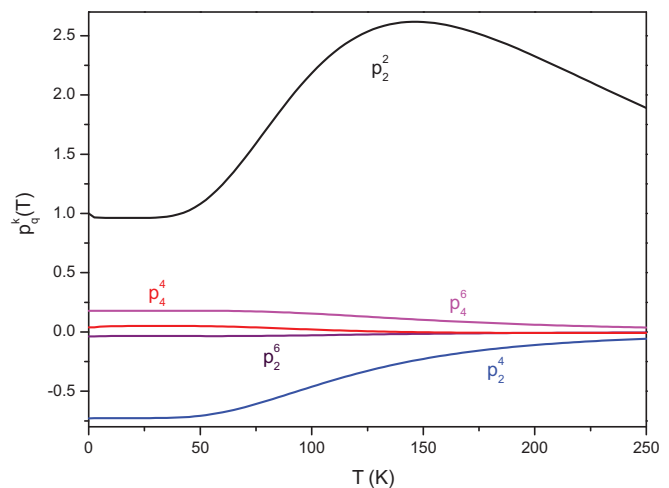


FIG. 6. (Color online) The dependencies of the relative contributions $p_q^k(T) = \frac{\langle C_q^k + C_{-q}^k \rangle_T}{\langle C_2^2 + C_{-2}^2 \rangle_0}$ to the polarization (10) on the temperature.

into account the influence of the magnetic field on the states of the Tb^{3+} ions.

The polarization is determined by

$$P_{\alpha}(H, T) = -\frac{\partial F_{me}}{\partial E_{\alpha}} = N \left[\frac{\sum_j \langle (\psi_j | D_{\alpha} | \psi_j) \rangle \exp(-\frac{E_j}{kT})}{\sum_j \exp(-\frac{E_j}{kT})} \right], \quad (9)$$

where the sums are taken over all the states $j = 1, \dots, 13$, and the D_{α} is a matrix of the chosen polarization operator. Using Eqs. (7), (8), and (9) the polarization P_x can be expressed in the form

$$P_x = d_2^2 \langle C_2^2 + C_{-2}^2 \rangle + d_2^4 \langle C_2^4 + C_{-2}^4 \rangle + d_2^6 \langle C_2^6 + C_{-2}^6 \rangle \\ + d_4^4 \langle C_4^4 + C_{-4}^4 \rangle + d_4^6 \langle C_4^6 + C_{-4}^6 \rangle, \quad (10)$$

where $d_q^k = N b_q^k$.

It follows from Eq. (10) that the dependencies of P_x on temperature and external magnetic field \vec{H} are determined by the thermal averages of operators $\langle C_q^k + C_{-q}^k \rangle$, where $k = 2, 4, 6, q = 2, 4$. The averages of operators $\langle C_q^k + C_{-q}^k \rangle$ have been calculated numerically as functions of H and T . It was established that $\langle C_q^k + C_{-q}^k \rangle$ for $H \perp z$ depends quadratically on the external magnetic field. They change sign when the orientation of the magnetic field is changed from $H || x$ to $H || y$. This is in complete agreement with the experimental data.

To describe the $P_x(T)$ behavior we have analyzed contributions of different multipoles $\langle C_q^k + C_{-q}^k \rangle$ and have ascertained a hierarchy of their magnitudes. The dependencies of the relative averages $p_q^k(T) = \frac{\langle C_q^k + C_{-q}^k \rangle_T}{\langle C_2^2 + C_{-2}^2 \rangle_0}$ are shown in Fig. 6. One can see that $p_4^4(T)$, $p_4^6(T)$ and $p_2^6(T)$ are significantly smaller in absolute value than $p_2^2(T)$ and $p_2^4(T)$.

As explained above, the experimental curve $P_x(T)$ can be accurately approximated by the expression (10) (see Fig. 5) that has only the first two terms $d_2^2 = -1.25 \times 10^5 \mu\text{C}/\text{m}^2$, $d_2^4 = -2.12 \times 10^5 \mu\text{C}/\text{m}^2$. The inclusion of the

rest of the harmonics with the coefficients d_q^k of the order of d_2^2 add only a weak contribution to P_x .

Theoretical and experimental data for the dependencies of electric polarization on the applied external magnetic field at different temperatures are shown in Figs. 3 and 4.

As in the case of rare-earth iron borates, the signs of longitudinal $P_a(H_a)$ and transverse $P_a(H_b)$ magnetoelectric effects at the same temperatures differ, which can be explained within the scope of the symmetry analysis of the crystals that belong to the space group $R32$ [17]. The dependencies of the electric polarization on magnetic field are quadratic ones similar to other rare-earth aluminum borates [11,12], but its temperature dependence reveals a nonmonotonous character. As shown in Fig. 5, the magnetically induced polarization has a relatively small but nonzero value at low temperatures, then it changes sign with the increase of T and reaches the value of $\approx 25 \mu\text{C}/\text{m}^2$ at high temperatures close to the room ones. The similar temperature dependence of polarization is observed in terbium iron borate [18].

The observed peculiarities of the terbium aluminum borates and iron borates can be explained by the fact that in both classes of the compounds the main contribution to magnetically induced polarization originates from the Tb^{3+} ions that are subjected to the external magnetic field (plus the f - d exchange field in the iron borate). The strongly anisotropic (Ising) nature of the ground state of the Tb^{3+} ion in the crystal plays a crucial role in the formation of the magnetoelectric properties and determines small (Van Vleck) susceptibility in the basal plane of the crystal and, correspondingly, a small field-induced polarization. The observed increase of polarization at high temperatures accompanied by the change of its sign can be explained by the contribution of the excited states of the Tb^{3+} ions. The temperature range (150–200 K), below which the polarization decreases and changes its sign, corresponds to the freezing of the nearest excited levels of Tb^{3+} in the crystal field at 200 cm^{-1} according to the optical data for $\text{TbAl}_3(\text{BO}_3)_4$ [20] and $\text{TbFe}_3(\text{BO}_3)_4$ [25].

It can be seen that B_n^k parameters obtained from spectroscopic data [20] allow to describe the dependence of polarization on the temperature and the external magnetic field.

IV. CONCLUSION

In this paper, we have presented both experimental and theoretical studies of the magnetic and magnetoelectric properties of terbium aluminum borate. A small electric polarization $P_a(H_{a,b})$ induced by magnetic field was observed at low (4 K) temperatures, which exhibits a sign change

and significant increase at high temperatures (150–300 K). In contrast to previous reports, our results show that the magnetoelectric effect in $\text{TbAl}_3(\text{BO}_3)_4$ is nonvanishing and has an anomalous temperature dependence. The magnetization and electric polarization increase monotonically with magnetic field. At low temperatures (below 50 K) a strong easy-axis magnetic anisotropy was observed (with c -axis magnetization saturated in low magnetic field < 10 kOe and in-plane magnetization depending linearly on the magnetic field), while at higher temperatures the anisotropy reduces significantly. The dependence of electric polarization on the external magnetic field in a wide temperature range is close to a quadratic function.

We demonstrated that the observed peculiarities of magnetic and magnetoelectric properties can be theoretically explained by the multipole moments of rare-earth Tb^{3+} ion. They were calculated taking into account the crystal field splitting of Tb^{3+} ground 7F_6 multiplet with the CF parameters B_n^k taken from the optical data. The influence of the two lower states with Van Vleck contribution of excited ones causes a small electric polarization. The anomalous temperature dependence of electric polarization is caused by the population of the upper levels with the increase of temperature. This is favorable for the realization of magnetoelectric properties in this material.

A comparison of the theory and experiment demonstrates good quantitative agreement and indicates that the parameters of crystal field obtained from studying spectroscopic data enable a precise description for both magnetic and magnetoelectric phenomena. Thus, the aluminum borates are model compounds for studying the contribution of rare-earth ions to the magnetoelectric properties by comparison of their properties with those of iron borates.

From a practical point of view, $\text{TbAl}_3(\text{BO}_3)_4$ has potential as a room temperature magnetoelectric material. Being an optical material as well, it is also interesting for the electromagneto-optical applications.

ACKNOWLEDGMENTS

We thank Dr. Daniel Sando for useful comments and remarks. This work is supported by the Russian Foundation for Basic Research (Projects No. 13-02-01093, No. 13-02-12443, No. 13-02-01093, No. 12-02-01261, and No. 13-02-12442) and a grant from the Russian Federation President on support of sciences schools no. 4828.2012.2, The Ministry of Education and Science of Russian Federation, Project No. 8365.

-
- [1] H. Schmid, *Ferroelectrics* **162**, 317 (1994).
 - [2] G. A. Smolenskii and I. E. Chupis, *Sov. Phys. Usp.* **25**, 475 (1982).
 - [3] I. E. Chupis, *ChemInform* **42** (2011).
 - [4] M. Fiebig, *J. Phys. D* **38**, R123 (2005).
 - [5] W. Eerenstein, N. D. Mathur, and J. F. Scott, *Nature (London)* **442**, 759 (2006).
 - [6] S.-W. Cheong and M. Mostovoy, *Nat. Mater.* **6**, 13 (2007).
 - [7] D. Khomskii, *Physics* **2**, 20 (2009).
 - [8] A. P. Pyatakov and A. K. Zvezdin, *Phys. Usp.* **55**, 557 (2012).
 - [9] A. K. Zvezdin, S. S. Krotov, A. M. Kadomtseva, G. P. Vorob'ev, and Y. F. Popov, *JETP Lett.* **81**, 272 (2005).
 - [10] A. K. Zvezdin, G. P. Vorob'ev, A. M. Kadomtseva, Y. F. Popov, A. P. Pyatakov, L. N. Bezmaternykh, A. V. Kuvardin, and E. A. Popova, *JETP Lett.* **83**, 509 (2006).
 - [11] K.-C. Liang, R. P. Chaudhury, B. Lorenz, Y. Y. Sun, L. N. Bezmaternykh, V. L. Temerov, and C. W. Chu, *Phys. Rev. B* **83**, 180417 (2011).

- [12] K.-C. Liang, R. P. Chaudhury, B. Lorenz, Y. Y. Sun, L. N. Bezmaternykh, I. A. Gudim, V. L. Temerov, and C. W. Chu, *J. Phys.: Conf. Ser.* **400**, 032046 (2012).
- [13] F. Kellendonk and G. Blasse, *J. Phys. Chem. Solids* **43**, 481 (1982).
- [14] C. B. Rubinstein, S. B. Berger, L. G. Van Uitert, and W. A. Bonner, *J. Appl. Phys.* **35**, 2338 (1964).
- [15] V. L. Temerov, A. E. Sokolov, A. L. Sukhachev, A. F. Bovina, I. S. Edel'man, and A. V. Malakhovskii, *Crystallogr. Rep.* **53**, 1157 (2008).
- [16] A. M. Kadomtseva, Yu. F. Popov, G. P. Vorob'ev, A. A. Mukhin, V. Yu Ivanov, A. M. Kuzmenko, and L. N. Bezmaternykh, *JETP Lett.* **87**, 39 (2008).
- [17] A. M. Kadomtseva, Yu. F. Popov, G. P. Vorob'ev, A. P. Pyatakov, S. S. Krotov, K. I. Kamilov, V. Yu. Ivanov, A. A. Mukhin, A. K. Zvezdin, A. M. Kuzmenko, L. N. Bezmaternykh, I. A. Gudim, and V. L. Temerov, *Low Temp. Phys.* **36**, 511 (2010).
- [18] A. K. Zvezdin, A. M. Kadomtseva, Yu. F. Popov, G. P. Vorob'ev, A. P. Pyatakov, V. Yu. Ivanov, A. M. Kuz'menko, A. A. Mukhin, L. N. Bezmaternykh, and I. A. Gudim, *JETP* **109**, 68 (2009).
- [19] A. M. Kadomtseva, Yu. F. Popov, G. P. Vorob'ev, K. I. Kamilov, V. Yu. Ivanov, A. A. Mukhin, and A. M. Balbashov, *JETP* **106**, 130 (2008).
- [20] I. Couwenberg, K. Binnemans, H. De Leebeeck, and C. Gorller-Walrand, *J. Alloys Compd.* **274**, 157 (1998).
- [21] A. I. Popov, D. I. Plokhov, and A. K. Zvezdin, *Europhys. Lett.* **87**, 67004 (2009).
- [22] N. V. Kostyuchenko, A. I. Popov, and A. K. Zvezdin, *Phys. Solid State* **54**, 1591 (2012).
- [23] A. I. Popov, D. I. Plokhov, and A. K. Zvezdin, *Phys. Rev. B* **87**, 024413 (2013).
- [24] M. N. Popova, T. N. Stanislavchuk, B. Z. Malkin, and L. N. Bezmaternykh, *Phys. Rev. B* **80**, 195101 (2009).
- [25] M. N. Popova, T. N. Stanislavchuk, B. Z. Malkin, and L. N. Bezmaternykh, *J. Phys.: Condens. Matter* **24**, 196002 (2012).